Closed-Loop Terrain Relative Navigation for AUVs with Non-Inertial Grade Navigation Sensors

Deborah K. Meduna[1], Stephen M. Rock[1,2], and Robert S. McEwen[2]

[1]Aeronautics and Astronautics, Stanford University, Palo Alto, CA
[2]Monterey Bay Aquarium Research Institute, Moss Landing, CA

***Abstract*—Terrain Relative Navigation (TRN) has the potential to enable drift-free, low-cost navigation for a wide range of underwater vehicles. Current underwater TRN systems have demonstrated meter-level navigation accuracy by utilizing high-accuracy inertial navigation systems in combination with both low and high quality sonar sensors and bathymetry maps. No studies, however, have considered the application of underwater TRN to vehicles with non-inertial-grade navigation systems, an extension which would greatly increase its applicability. The use of low-grade motion sensors in TRN is problematic due to the presence of large errors which can cause highly inaccurate alignment of successive sonar pings. To address this, a TRN filter is developed in which information present in the terrain correlations is used to help identify and mitigate large motion sensor errors. The resulting filter consists of a tight coupling between TRN and the onboard navigation, yielding a significantly improved navigation solution. The development of this TRN system is detailed for an AUV with an Attitude, Heading and Reference System (AHRS)-based dead reckoning navigation, which has an observed accuracy of $5-25\%$ distance traveled. Field trials in Monterey Bay, CA demonstrate the ability of the TRN filter to acheive $5-10m$ navigational precision. Field trials are also presented demonstrating successful real-time, closed-loop TRN on the AUV. For these trials, the combined TRN/AHRS system enabled the vehicle to fly to a known beacon location with ability comparable to an acoustic homing system. The presented results demonstrate that TRN technology can successfully be applied to non-inertial-grade vehicle platforms, greatly improving the navigation capabilities of such systems.**

I. Introduction

Terrain Relative Navigation (TRN) can enable drift-free, low-cost navigation for underwater vehicles, providing a powerful alternative to other absolute navigation methods such as periodic resurfacing for GPS and acoustic navigation (e.g. USBL, LBL). TRN produces vehicle position estimates by matching range measurements of the terrain against an a priori terrain map. The technology was initially developed for use on aerial vehicles, originating with the cruise missile guidance system TERCOM (Terrain Contour Matching) which utilized batch correlation of altimeter measurements against a topography map [1].

Since TERCOM, many variants of TRN have been developed for numerous platforms, with a growing interest over the last decade in application to underwater vehicles. This recent development of underwater TRN algorithms has been largely focused on TRN's ability to reduce accumulated inertial drift errors, replacing or augmenting the use of more traditional GPS and/or acoustic navigation systems [2], [3], [4], [5], [6].

All of these current implementations of underwater TRN have achieved high accuracy (meter-level) performance by utilizing high accuracy inertial navigation systems ($\leq 1\%$ drift rates) in combination with high quality sonars and/or terrain maps. For example, TRN systems on the HUGIN [3], Autosub6000 [7], and Dorado AUVs [5] have all utilized multibeam sonar sensors, while an area sonar has been used for TRN on the AUV62f [6]. Using such high quality sonar sensors allows for the acquisition of information-rich measurements of the terrain, which can greatly improve TRN performance. However, meter-level accuracy with TRN has only been achieved by further incorporating a high-quality Inertial Navigation System (INS), which provides highly accurate measurements of the relative spacing and orientation of sonar pings.

The reliance of existing underwater TRN systems upon such highly accurate sensors severely limits the vehicles to which they can be applied. To address this concern, recent work has studied the performance trades associated with using lower quality sensors and maps for TRN. In [8], it was shown that lower-quality sonar sensors (e.g. Doppler Velocity Log (DVL) or Altimeter sonars), in combination with a highly accurate INS, could achieve meter-level TRN navigation accuracy at the expense of slower estimator convergence. In [9], it was further shown that TRN could achieve sub-map-resolution navigational accuracies, indicating that high-resolution maps, while beneficial, are not critical for TRN applications. However, no studies currently exist on the effect of utilizing non-inertial-grade motion sensors for TRN, where navigation errors accrue at $\geq 5\%$ distance traveled.

Low-grade navigation systems are problematic for TRN due to the presence of large sensor errors which results in highly inaccurate alignment of successive sonar pings. These errors generally arise from specific sensor biases or misalignments which, unless accounted for, can yield large biases in the TRN and onboard navigation estimates. Fortunately, information present in the terrain correlations from TRN can aid in the identification and mitigation of these sensor errors, resulting in a significantly improved navigation solution. This concept is closely related to the use of GPS for error identification in low-cost IMUs on aerial and land vehicles [10], [11].

In order to exploit the capability of TRN to reduce the errors introduced by low-grade navigation systems, several changes to traditional TRN systems must be made. First, the estimated state must be augmented to include motion sensor errors. This

state augmentation consequently requires higher-dimensional estimators than the $2-3$ state estimators traditionally used for underwater TRN. Finally, a new framework is needed for combining TRN with the onboard navigation which will allow direct fusion of raw sensor measurements into the TRN filter.

This paper details the development of such a TRN system for an AUV with an Attitude, Heading and Reference System (AHRS)-based navigation system with an observed accuracy of $5-25\%$ distance traveled. The presented TRN implementation utilizes an 8-dimensional particle filter for estimating critical motion sensor errors observed in the vehicle. A TRN/AHRS integration framework is then developed which incorporates motion sensor information directly into the TRN algorithm. The resulting integrated TRN/AHRS navigation system is demonstrated in real-time field trials in Monterey Bay, CA. Results from both open and closed loop tests are presented, showing that the proposed filter enabled $5-10m$ navigational precision on the AUV along with a return-to-site capability comparable to an acoustic homing system. The results demonstrate the ability to utilize TRN technology successfully on non-inertial-grade platforms, significantly improving the navigation capabilities of such systems.

II. Test Platform

The algorithms presented in this paper were developed for and tested on the Benthic Imaging AUV (BIAUV), operated by the Monterey Bay Aquarium Research Institute (MBARI). The vehicle, pictured in Fig. 1, has been developed by MBARI for the purpose of generating visual mosaics of sites of interest on the seafloor.

Table I shows a list of the vehicle's navigation sensors and specifications. Using these sensors, the BIAUV typically navigates through a combination of three modes: (i) GPS-based navigation when the vehicle is on the surface, (ii) acoustic-based homing to a beacon when in range, and (iii) dead-reckoning (primary mode). Under dead-reckoning, the vehicle utilizes attitude measurements from the AHRS and integrated DVL-measured velocities to estimate vehicle motion. This dead-reckoning system is rated at an accuracy of $\approx 5\%$ distance-traveled (DT). Consequently, the BIAUV's navigation system falls under the classification of non-inertial-grade.

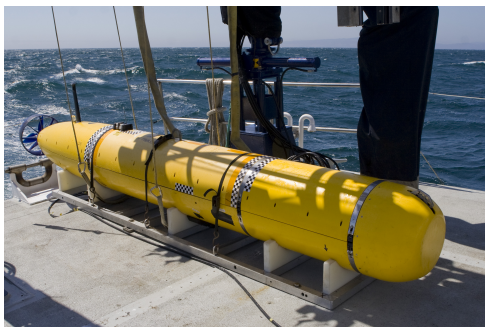

Fig. 1. Picture of the MBARI Benthic Imaging AUV (BIAUV). Photo courtesy of Peter Kimball.

TABLE I
BIAUV Navigation Sensor Specifications

INSTRUMENT	MODEL	VARIABLE	SPECS
Altimeter	Imagenex 881	Altitude	2.1^o beamwidth
Pressure Sensor	Paroscientific	Depth	0.01%
AHRS	Microstrain 3DM-GX1	Attitude Angular Rate	$\pm 2^o$ $3.5^o/\sqrt{hr}$ RW
$300kHz$ DVL	RDI Workhorse Navigator	Range Velocity	4^o beamwidth $\pm 0.4\% \pm 0.2\frac{cm}{sec}$
Acoustic Ranger	Sonardyne Scout USBL	Range-To-Beacon	$\pm 2.75\%$ slant range
GPS	Ashtech	Position	-

For non-inertial-grade vehicles, the sources of navigation error are highly platform dependent, arising from a combination of sensor-specific errors and misalignments. For the BIAUV, the primary source of navigation error was traced to magnetic compass errors in the vehicle's AHRS. Fig. 2 shows the compass measurements for a field test in February, 2010, compared against the best estimate of true heading derived from ship-based USBL tracking. This estimate was computed by finding the heading which best translated DVL-measured vehicle velocity into the USBL-measured inertial velocity (estimated from a kernel-smoothed USBL track).

As Fig. 2 shows, the AHRS and USBL heading estimates differ significantly, indicating compass errors as large as $30-40^o$. In this trial, these compass errors resulted in an observed navigational accuracy of $\approx 25\%DT$, much worse than specifications. While the observed compass errors were believed to be a result of poor magnetic calibration, further calibrations failed to significantly improve the AHRS heading accuracy.

III. TRN Algorithm

For vehicles with inertial-grade navigation sensors, low-dimensional TRN filters are commonly employed with linear

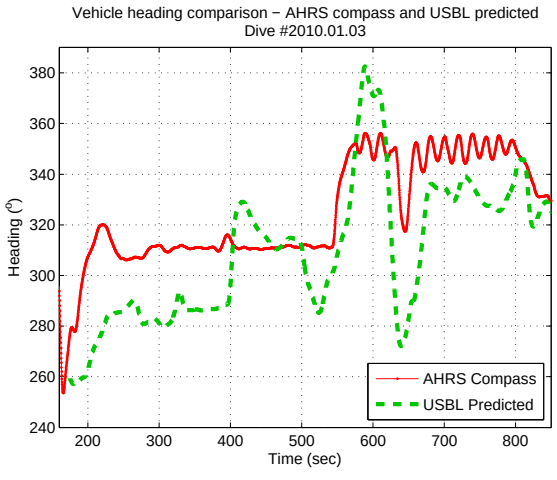

Fig. 2. Comparison of heading estimates from AHRS compass (red,solid) and the smoothed USBL track (green,dashed) for a section of a BIAUV dive on 02/10/10. Note that the two estimates of heading differ by $> 25^o$ for much of this portion of the dive.

motion updates based on INS position measurements. The large inaccuracies inherent in low-grade navigation sensors, however, require a higher-dimensional estimation state and corresponding estimator.

A. Process Model

The design of a TRN system for a non-inertial-grade platform should reflect the platform-specific distribution of errors. For the BIAUV, the primary errors were associated with the compass, making it essential to incorporate additional filter states for separately estimating heading based upon gyroscope measurements. Furthermore, the low-grade of the AHRS sensor motivated the additional inclusion of roll and pitch in the estimated state. The resulting estimation state vector for the system is 8-dimensional:

$$\mathbf{x} = \begin{bmatrix} \mathbf{p} & \mathbf{q} & \omega_y^b & \omega_z^b \end{bmatrix}^T \tag{1}$$

where $\mathbf{p} = \begin{bmatrix} x_N & x_E & z \end{bmatrix}$ and $\mathbf{q} = \begin{bmatrix} \phi & \theta & \psi \end{bmatrix}$ are the position and attitude vectors of the vehicle, and ω_y^b and ω_z^b are the gyroscope biases for the y and z components of the vehicle's angular rates. It was not necessary to estimate the gyroscope bias in the x component of angular rate, as roll and pitch could be updated directly with AHRS measurements (i.e., without integrating angular rates).

The resulting process model is given by:

$$\boldsymbol{x}_{k+1} = \boldsymbol{x}_k + \left\{ \begin{array}{l} \begin{bmatrix} 1 & 0 & 0 \\ 0 & 1 & 0 \end{bmatrix} R(\hat{\mathbf{q}}_k)\boldsymbol{v}_k dt \\ \Delta z_k \\ \Delta\phi_k \\ \Delta\theta_k \\ \begin{bmatrix} \frac{\sin\hat{\phi}_k}{\cos\hat{\theta}_k} & \frac{\cos\hat{\phi}_k}{\cos\hat{\theta}_k} \end{bmatrix} \left\{ \begin{array}{l} \omega_{y,k} - \hat{\omega}_{y,k}^b \\ \omega_{z,k} - \hat{\omega}_{z,k}^b \end{array} \right\} dt \\ \mathbf{0}_2 \end{array} \right\} + \boldsymbol{r}_k \tag{2}$$

where $R(\hat{\mathbf{q}}_k)$ is the rotation matrix for the current attitude estimate, $\boldsymbol{v}_k$ is the DVL measured velocity in the vehicle frame, Δz_k, $\Delta\phi_k$ and $\Delta\theta_k$ are the change in depth, roll and pitch measured by the pressure depth and AHRS sensors, $\omega_{y,k}$ and $\omega_{z,k}$ are the vehicle angular rates measured by the AHRS, and $r_k \sim \mathcal{N}(0, \Sigma_r)$ is the process noise.

In (1) and (2), the states $\boldsymbol{q}$, ω_y^b and ω_z^b have been included entirely as a result of the low-accuracy of the navigation sensors on the BIAUV. In comparison, TRN systems with high-accuracy inertial systems typically only estimate the position vector, $\boldsymbol{x} = \boldsymbol{p}$, and incorporate a linear motion update based on the INS estimate of position: $\boldsymbol{p}_{k+1} = \boldsymbol{p}_k + \Delta\boldsymbol{p}_k^{INS} + r_k$. This type of simplified filter was utilized in [9], for example, for TRN on an AUV with an inertial navigation accuracy $< 0.05\%DT$. By utilizing the low-accuracy motion sensors on the BIAUV, the estimation state vector has grown in size by five dimensions and the process model has become nonlinear.

B. Observation Model

The observation model for the TRN measurements is given by:

$$\boldsymbol{y}_k = h(\boldsymbol{x}_k) + e_k \tag{3}$$

where $\boldsymbol{y}_k \in \mathcal{R}^N$ contains the N projected sonar measurements of terrain depth, $h(\boldsymbol{x}_k)$ is the corresponding terrain depth at the sonar projected beam locations, and $e_k \sim \mathcal{N}(0, \Sigma_e)$ is the sonar measurement noise.

Since the true terrain surface is not generally known, the terrain function $h(\boldsymbol{x}_k)$ must be approximated by a model. Typically, a Digital Elevation Model (DEM) is used in which the terrain is represented by a grid of elevation values equally distributed in North and East. In order to estimate the terrain depth at any location, an interpolation method on the DEM is utilized. The resulting terrain function in (3) is then replaced by:

$$\begin{aligned} h_i(\boldsymbol{x}_k) &= \hat{h}_i(\boldsymbol{x}_k) && (4) \\ &= \lambda^T h_i^M[\boldsymbol{x}_k] + \nu_{i,k} && (5) \end{aligned}$$

where $h_i^M[\boldsymbol{x_k}]$ is a vector of DEM values in the neighborhood of the projected measurement $y_{i,k}$, λ is a set of interpolation weights, and $\nu_{i,k}$ is the DEM modeling error. The variance of $\nu_{i,k}$ is a combination of the uncertainty in the original DEM along with uncertainty associated with the interpolation. The details of this calculation are described in [9].

Assuming that the sonar measurement noise is uncorrelated with the map error and errors between beams are independent, the probability of acquiring the current sonar measurement, $\boldsymbol{y}_k$, given vehicle state $\boldsymbol{x}_k$ is given by:

$$p(\boldsymbol{y}_k|\boldsymbol{x}_k) = \alpha \exp\left(-\frac{1}{2} \sum_{i=0}^{N} \beta_i \left[y_{i,k} - \hat{h}_i(\boldsymbol{x}_k) \right]^2 \right) \tag{6}$$

where

$$\beta_i = \frac{1}{\sigma_{i,e}^2 + \sigma_{i,\nu}^2}. \tag{7}$$

Due to the natural nonlinearity of the terrain function, $\hat{h}(\boldsymbol{x})$, the likelihood surface in (6) is highly nonlinear in the state, and increases in nonlinearity with fewer measurement beams.

C. Filter Implementation

The non-linearity of the described process and observation models motivates the use of a full Bayesian, non-parametric filter for successfully tracking the vehicle state estimate. In [9], the authors utilized a point mass filter (PMF), or histogram filter, for state propagation due to its known higher robustness over other non-parametric methods for low-dimensional problems [12]. However, the increase in the number of states needed for the presented filter motivated a shift to a particle filter implementation.

A particle filter is a sampled-based approximation to the general Bayesian filter equations:

$$\begin{aligned} p(x_k|y_{k-1}) &= \int p(x_k|x_{k-1}) p(x_{k-1}|y_{k-1}) \\ p(x_k|y_k) &= \alpha p(y_k|x_k) p(x_k|y_{k-1}). && (8) \end{aligned}$$

More specifically, in a Particle Filter (PF), the probability densities in (8) are represented by a set of state-space samples with corresponding weights, called the particle set: $\{x^{[m]}, w^{[m]}; m = 1...N\}$. The density and weights of these samples are selected such that integrating the weighted samples over a region of the state-space will yield the corresponding integral of the true probability density for that same region.

By using this particle-based approximation, the sample distribution can adjust to a particular probability density, increasing the concentration of particles in higher-probability regions of the state-space. In general, this allows for more efficient and cost-effective representation of probability densities than methods like the PMF, reducing the impact of increased state dimension.

Over the last decade, particle filters have grown in popularity for a variety of applications, particularly in mobile robotics. For a more in-depth overview of particle filters, see [13], [14] and [15]. The particle filter formulation used for the presented algorithm is a Sampling Importance Resampling (SIR) filter, also known as a Bayesian bootstrap filter [16]. The only modification is the use of effective sample size, $\hat{N}_{eff} = 1/\sum_{m=1}^{N}(w^{[m]})^2$, as a criterion for particle resampling, as described in [15]. This standard PF implementation proved sufficient for accurately propagating the probability densities associated with the presented TRN system.

IV. TRN/AHRS Integration

In addition to the increased complexity of the TRN filter, as described in the previous section, the use of low-grade motion sensors further impacts the approach for integrating the TRN and onboard navigation systems. When the onboard navigation system is highly accurate, a loosely coupled integration scheme works well in which (i) the filtered output of an INS is used as input to the TRN filter, and (ii) a central Kalman Filter is used to fuse the resulting INS and TRN filter estimates. This integration method is typical of what has been utilized in other fielded underwater TRN systems [17],[18].

Such loosely-coupled systems have also been the primary focus of TRN/INS integration studies, which have considered only different mechanisms for representing the TRN estimate prior to combining it in a central filter with INS [19]. The SITAN framework [20] provides an alternative in which range measurements and linearized terrain correlations are fused into a central INS filter, typically an Extended Kalman Filter. However, due to the linearizations involved, this framework is only applicable to systems with highly accurate inertial navigation.

The use of non-inertial-grade onboard navigation systems thus requires a new integration approach. In particular, as seen by the process model developed in Section III-A, the use of low-accuracy motion sensors requires a framework in which unfiltered sensor data is directly fused into a central TRN filter. Fig. 3 shows a graphic of this resulting integration framework, denoted tight-TRN-integration, for the BIAUV.

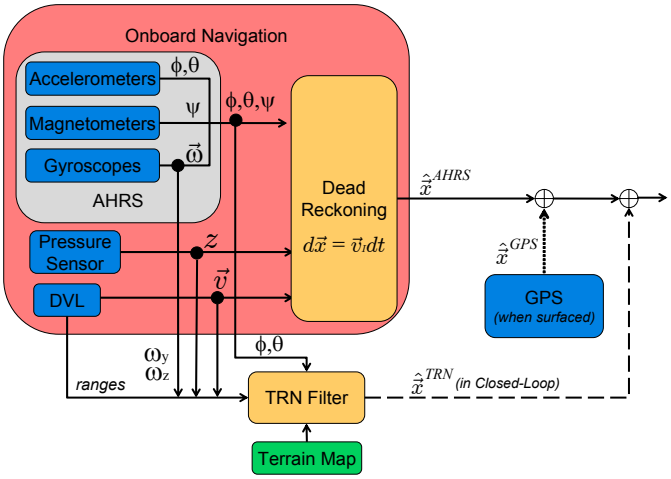

Fig. 3. Block Diagram showing the tight-TRN-integrated navigation system implemented on the BIAUV.

Algorithm 1 TRN/AHRS Closed-Loop Navigation Algorithm

$\Delta \boldsymbol{p}_{corr} = \mathbf{0}$
for all t **do**
  $\delta = \hat{\boldsymbol{p}}_t^{AHRS} - \hat{\boldsymbol{p}}_t^{TRN}$
  if $(|\delta| \leq \Delta_{MAX})$ & $(\sigma(\hat{\boldsymbol{p}}_t^{TRN}) \leq S_{MAX})$ **then**
    $\Delta \boldsymbol{p}_{corr} = \delta$
  end if
  $\hat{\boldsymbol{p}}_t^{AHRS} = \hat{\boldsymbol{p}}_t^{AHRS} + \Delta \boldsymbol{p}_{corr}$
end for

A. Implementation

Despite the improved navigational accuracy of the resulting TRN/AHRS filter, the TRN estimate is only utilized for vehicle navigation and control when it is sufficiently accurate. For the deployed system, this accuracy requirement is defined by a maximum estimate variance, S_{MAX}, and a maximum estimate offset from the onboard navigation, Δ_{MAX}. When the TRN filter estimates do not meet these constraints, the onboard navigation estimates are used instead (corrected by the last valid TRN filter estimate). Such a system ensures that the TRN filter is not used in conditions where it has poor performance (e.g. over flat terrain), while maintaining its primary role in the overall vehicle navigation.

For simplicity in implementation, the TRN estimates are incorporated into the BIAUV's navigation by applying associated corrections to the onboard navigation. This process is similar to a GPS correction, but occurs continuously. The method effectively sets the onboard navigation estimate equal to the TRN estimate when the TRN filter is performing well, and ensures that the onboard navigation starts with zero drift error when it becomes primary. Algorithm 1 describes this navigation update process utilized on the BIAUV, where $\Delta \boldsymbol{p}_{corr}$ is the TRN estimate correction to the onboard navigation. For the current deployed system, this correction only includes north and east position states.

V. Field Demonstrations

The performance of the described integrated TRN/AHRS navigation system was demonstrated through a series of field trials in Soquel Canyon, Monterey Bay, CA on the Benthic Imaging AUV described in Section II. Both open-loop and closed-loop tests were performed. In open-loop testing, the vehicle utilized the onboard navigation as the primary navigation system, while the closed-loop testing incorporated real-time TRN corrections as described in Section IV-A.

For all of the field trials, the TRN filter was run with an initial search area of $\pm 60m$ in North and East and a resampling criteria of $\hat{N}_{eff} = 0.75N$. Terrain correlations in the TRN algorithm were performed using the BIAUV's DVL sonar range measurements and a 1m-resolution bathymetry map generated by MBARI's Mapping AUV. Sensor error uncertainty values were selected in correspondence with the sensor specifications in Table I. The filter was run at an update rate of $\approx 0.3Hz$, resulting in filter updates approximately every 4.5 meters. Utilizing this update rate ensured that successive sonar measurements were non-overlapping, allowing them to be considered independent.

The inaccuracy of the onboard navigation system and the lack of an external positioning system (e.g. LBL array) motivated the use of a non-traditional method of acquiring truth in these trials for validating the TRN navigation estimates. In particular, for all field trials, trajectories were planned towards a known beacon location, allowing the vehicle to take homing measurements of a common reference point for all missions. The estimated location of the homer could then be compared between different runs, and the precision determined by the consistency of the different estimates. The following section details the calculation of these homer location estimates.

A. Homer Location Estimation

For each field trial, the BIAUV used its homing system to take vehicle-relative position measurements of a beacon deployed in Soquel Canyon. In order to translate these measurements into inertial estimates of the homer location, both attitude and position estimates of the vehicle are needed. Equation (9) shows this conversion

$$\hat{\boldsymbol{p}}_h = \hat{\boldsymbol{p}}_v + \hat{R}_{Iv}\boldsymbol{\rho}^v_{vh} \tag{9}$$

where $\hat{\boldsymbol{p}}_h$ and $\hat{\boldsymbol{p}}_v$ are the estimated homer and vehicle locations in inertial coordinates, $\hat{R}_{Iv}$ is the estimated vehicle rotation matrix, and $\boldsymbol{\rho}^v_{vh}$ is the measured relative location of the homer to the vehicle in the vehicle-frame. Note that it has been assumed that the homing system is collocated with the vehicle's navigation sensors.

Since the TRN filter is implemented as a particle filter, the evaluation of (9) results in a particle distribution over the homer location. The m^{th} particle in this distribution is drawn as follows::

$$\begin{aligned} \boldsymbol{p}_h^{[m]} &\sim \mathrm{p}(\boldsymbol{p}_h|\boldsymbol{x}, \boldsymbol{\rho}^v_{vh}) \\ &= \boldsymbol{p}_v^{[m]} + R_{Iv}^{[m]}(\boldsymbol{\rho}^v_{vh} + e_\rho) \end{aligned} \tag{10}$$

where $e_\rho \sim \mathcal{N}(0, \sigma_\rho)$ is the error on the homing measurement. The estimated homer location, $\hat{\boldsymbol{p}}_h$, can then be calculated as the mean of this resulting particle distribution.

While the homing system provided multiple measurements over the course of each vehicle run, only one measurement per trial was utilized in evaluating (10). The measurement selected was that associated with the vehicle's closest approach to the beacon, prior to passing over it. As the TRN algorithm had converged at this point in the trajectory for all of the presented vehicle runs, the probability distribution over homer location could reasonably be approximated by a Gaussian with mean and variance computed from the particle set.

Utilizing this methodology for estimating homer location, the presented TRN system was validated through a series of open-loop and closed-loop tests, demonstrating significant improvements to the onboard navigation.

B. Open-Loop testing

In open-loop testing, the vehicle was flown on several different trajectories in which its homing capability was used to approach the fixed homer location. In each of these runs, the onboard navigation was used as the primary navigation system (i.e. TRN corrections were not employed). Fig. 4 shows a graphic of five of the trajectories overlaid onto the bathymetry map used in the TRN algorithm, estimated from USBL ship-based tracking. The trajectories were flown during field tests in October, 2009 and February, 2010. For each of these runs, the vehicle was able to home to within $10 - 20m$ laterally of the beacon at an altitude of $\approx 50m$.

Using (10), homer location estimates were generated in post-processing for each of the runs for both the TRN filter and the onboard navigation, using 40,000 particles. The results are shown in Fig. 5. As the figure clearly shows, the TRN filter estimates of the homer location are significantly more consistent than the onboard navigation estimates. The spread of the TRN estimates across all five runs is $\approx 9m$ in North and $\approx 7m$ in East, compared with $\approx 160m$ in both North and East for the onboard navigation.

As Fig. 5 also shows, the estimated homer location given by TRN is offset from the a-priori estimated location by $\approx 18m$ in North and $\approx 5m$ in East. This apparent offset can be primarily accounted for by geo-registration errors in the reference map. As discussed in [9], significant geo-registration errors on the order of $20 - 40m$ have been observed for $1m$ resolution bathymetry maps in Monterey Bay, including maps of the Soquel Canyon site. Geo-registration errors computed for the current map showed good agreement with the estimated homer location offset.

The above results clearly demonstrate the precision of the TRN filter as compared with the onboard navigation. In order to evaluate the accuracy of the presented system across an entire run, the filter estimates were further compared with ship-based USBL vehicle tracking. Fig. 6 shows a comparison of the TRN filter estimated vehicle track, the smoothed ship-based USBL track, and the onboard navigation track for one of

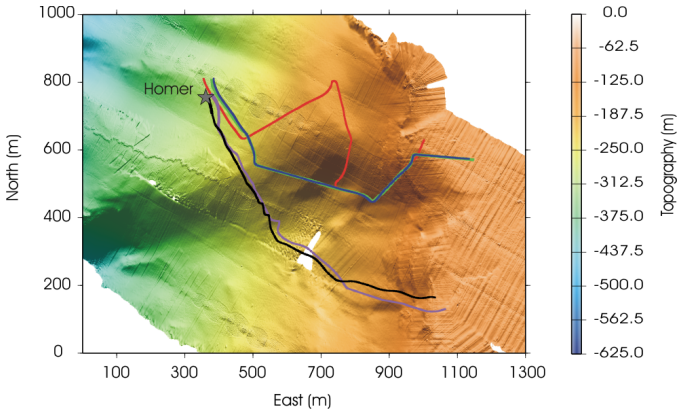

Fig. 4. Soquel Canyon 1m resolution bathymetry map near homer, overlaid with estimated vehicle trajectories from five runs of the BIAUV in the 10/20/09 and 02/10/10 field trials.

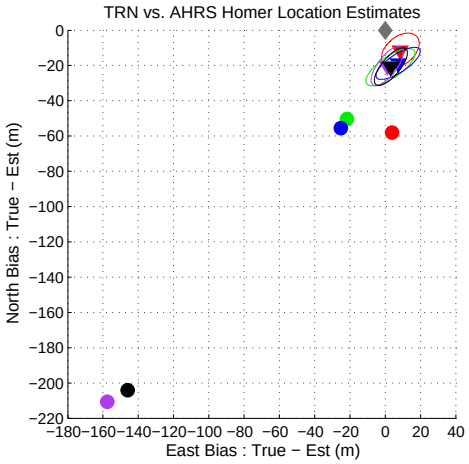

Fig. 5. Onboard navigation and TRN filter estimates of the homer location, relative to the a-priori homer location (at the origin). Circles indicate onboard navigation estimates, while the triangles and ellipses represent the TRN filter estimates along with the corresponding 90% confidence ellipse. Colors are coordinated with the color of the vehicle tracks in Fig. 4.

the runs from Fig. 4. As the figure demonstrates, the TRN estimate significantly outperforms the onboard navigation, closely following the USBL predicted vehicle track and correctly indicating that the vehicle flew directly to the homer.

In addition to improving vehicle position estimates, the TRN filter further produced improved vehicle attitude estimates, particularly in heading. Fig. 7 shows the heading estimates for a section of the run shown in Fig. 6, corresponding with the heading error plot shown earlier in Fig. 2. The figure shows the onboard compass measurements, the heading estimate derived from the USBL track, and the TRN heading estimate. The TRN estimated heading clearly follows the USBL prediction much more closely than the onboard compass, indicating that the filter significantly improved the estimation of this variable in the navigation. This improved heading estimate was critical to the overall improved navigation obtained with TRN on this particular vehicle.

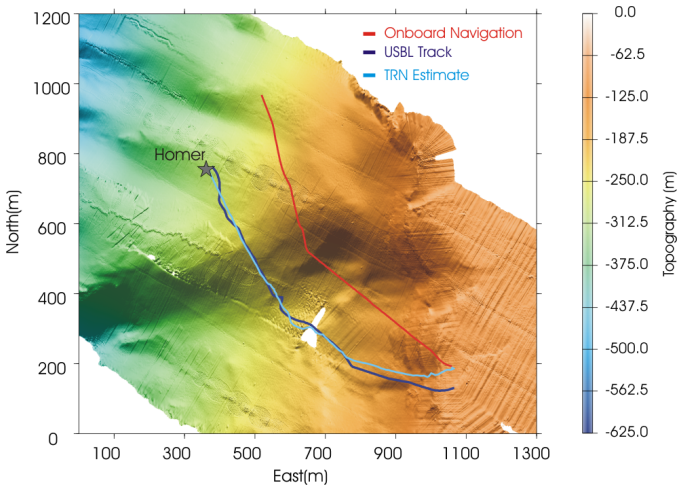

Fig. 6. Soquel Canyon 1m resolution bathymetry map, overlaid with onboard navigation, TRN, and USBL estimated vehicle trajectories from one run of the 02/10/10 field trials on the BIAUV.

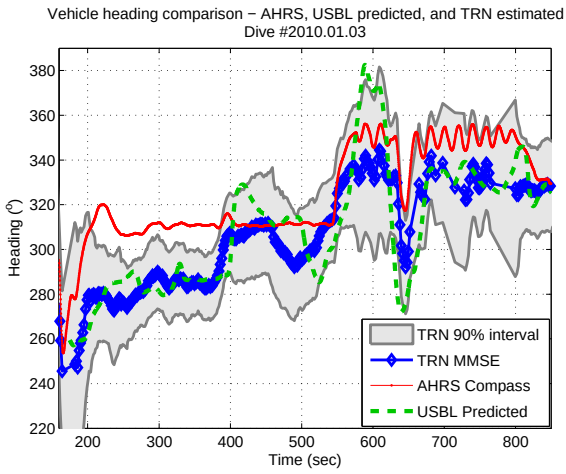

Fig. 7. Comparison of vehicle heading estimates from a portion of a BIAUV run shown in Fig. 6. Shown are the TRN mean estimate with 90% confidence bound, the onboard navigation estimate from the AHRS, the USBL (near-truth) predicted vehicle direction, and the commanded heading. Note that the onboard estimate and USBL estimate differ by as much as 25^o, whereas the TRN estimate aligns well with the USBL prediction.

C. Closed-Loop testing

In March, 2010, the TRN/AHRS integrated system was utilized for real-time closed-loop navigation of the BIAUV. For this closed-loop testing, the vehicle was flown on a trajectory toward the homer in which homing measurements were taken but were *not* utilized in navigating the vehicle. For this test, the filter integration parameters were $S_{MAX} = 30m^2$ and $\Delta_{MAX} = 300m$. The filter was run with 3,000 particles in order to minimize the load on the vehicle's CPU, a LiPPERT Cool SpaceRunner 2 with $300MHz$ processor speed and $128MB$ SDRAM.

Fig. 8 shows the results of this closed-loop test. Plotted are the uncorrected onboard navigation (red), the TRN/AHRS integrated filter solution (light blue), and the TRN/AHRS-

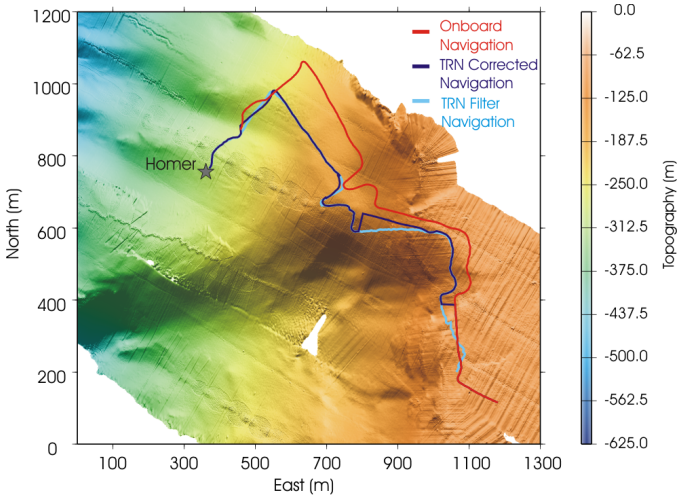

Fig. 8. Results from the 03/30/10 field demonstration of closed-loop TRN navigation on the BIAUV. The estimated vehicle trajectory is shown over a 1m-resolution map of Soquel Canyon for: the onboard (uncorrected) navigation, the TRN filter, and the TRN corrected navigation (used in the vehicle control). By flying with TRN corrections, the vehicle was able to successfully fly directly to the homer, whereas the raw onboard navigation would have left the vehicle 140m short of the goal.

corrected navigation solution (dark blue). As the figure shows, the TRN-corrected navigation solution brings the vehicle directly toward the homer, whereas the uncorrected onboard navigation would have stopped the vehicle far short of the beacon. Specifically, using the homing measurements, the vehicle was found to be $35m$ laterally from the homer when the corrected navigation solution indicated the vehicle was directly overhead. By comparison, the uncorrected onboard navigation at the same time placed the vehicle $140m$ away from the expected homer location.

The inability of the TRN-corrected navigation to fly the vehicle directly over the homer in this test can be partially attributed to an error in the mission programming, which sent the vehicle to the homer's inertial location rather than its geo-referenced location. Accounting for the predicted geo-referencing offset from the open loop trials, the expected lateral range to the beacon would have been $\approx 23m$, near what was achieved by the homing system in the open-loop trials.

Finally, Fig. 8 also demonstrates the occasional differences that can arise between the integrated TRN filter and the TRN-corrected navigation filter solutions as a result of the accuracy checks employed on the TRN estimates (Algorithm 1). Deviations between the two solutions can be seen both at the start of the run and at several later points in the mission. The former case corresponds to the initialization stage when the TRN filter is converging, while the latter corresponds to times when the vehicle experienced prolonged losses of DVL measurements, resulting in growing uncertainty in the TRN filter.

The presented results demonstrate the ability of the integrated TRN system to significantly improve the online navigation performance of the BIAUV, enabling return-to-site capabilities without the use of a homing system.

VI. Conclusion

The presented algorithms and results demonstrate that TRN can be successfully applied to vehicles with low-grade navigation sensors, providing significant navigation improvements over simple dead-reckoning systems. In particular, field trials on an AUV with dead-reckoning navigational accuracy of $5 - 25\%DT$ demonstrated the ability of TRN to provide $5 - 10m$ navigational precision and an online return-to-site capability comparable to an acoustic homing system.

For the AUV utilized in the presented work, the dominant error in the low-accuracy motion sensors was shown to arise from the vehicle compass. Accordingly, the designed TRN algorithm incorporated additional states to allow heading estimation through angular rate integration. Indeed, the resulting TRN filter produced significantly improved heading estimates, a critical component to the overall achieved navigational accuracy.

While the presented TRN system was developed for a particular vehicle, the employed integrated TRN filter is applicable and beneficial to any non-inertial-grade vehicle. Regardless of the platform-specific sources of navigational error, the use of low-grade motion sensors for TRN will require a shift to both a high-dimensional estimator and a tight-TRN-integration framework similar to that presented in this work.

Thus, the results in this paper suggest that TRN can be successfully applied to vehicles with non-inertial-grade sensors, achieving significant performance improvements over their nominal navigation systems. While the use of inertial-grade sensors will certainly improve TRN performance, non-inertial-grade vehicles using TRN can still achieve return-to-site navigation with $5 - 10m$-level navigational precision.

Acknowledgment

The authors would like to thank MBARI for support and the Stanford Graduate Fellowship for partial funding of this work. Researchers at MBARI who were particularly invaluable in acquiring the presented data include Dave Caress, Brett Hobson, Hans Thomas, Doug Conlin, Brian Schlining and Duane Thompson.

References

[1] Joe P. Golden, "Terrain countour matching(tercom): a cruise missile guidance aid," *SPIE*, vol. 238, pp. 10–18, 1980.

[2] Johan Carlstrom, "Results from sea trials of the swedish auv62fs terrain navigation system," in *UUST '07: Unmanned Untethered Submersible Technology*. Saab Underwater Systems, 2007.

[3] B. Jalving and O.K. Mandt, M. Hagen, "Terrain referenced navigation of auvs and submarines using multibeam echo sounders," in *UDT '04*, Nice, France, June 2004, Norwegian Defence Res. Establ.

[4] R. Karlsson and F. Gustafsson, "Bayesian surface and underwater navigation," *IEEE Transactions on Signal Processing*, vol. 54, no. 11, pp. 4204, 2006.

[5] Nathaniel Fairfield and David Wettergreen, "Active localization on the ocean floor with multibeam sonar," in *OCEANS '08: Oceans, Poles and Climate: Technological Challenges*, Quebec City, Quebec, September 2008.

[6] Ingemar Nygren, "Robust and efficient terrain navigation of underwater vehicles," in *IEEE/ION Position, Location and Navigation Symposium*, 2008, pp. 923–932.

[7] C. Morice, S. Veres, and S. McPhail, "Terrain Referencing for Autonomous Navigation of Underwater Vehicles," in *Proceedings of IEEE OCEANS '09*, Bremen, 2009.

[8] Deborah Meduna, Stephen Rock, and Rob McEwen, "Low-cost terrain relative navigation for long-range auvs," in *OCEANS '08: Oceans, Poles and Climate: Technological Challenges*, Quebec City, Quebec, September 2008.

[9] Deborah Meduna, Stephen Rock, and Robert McEwen, "Auv terrain relative navigation using coarse maps," in *UUST '09*, August 2009.

[10] S. Godha, "Performance evaluation of low cost MEMS-based IMU integrated with GPS for land vehicle navigation application," M.S. thesis, Department of Geomatics and Engineering, Univertisy of Calgary, 2006.

[11] Rudolph van der Merwe and Eric Wan, "Sigma-point kalman filters for integrated navigation," in *Proceedings of the 60th Annual Meeting of the Institute of Navigation (ION)*. Adaptive Systems Lab OGI School of Science & Engineering, 2004, pp. 641–654.

[12] Kjetil Bergh Anonsen and Oddvar Hallingstad, "Terrain aided underwater navigation using point mass and particle filters," in *IEEE PLANS*, April 2006, pp. 1027–1035.

[13] Sebastian Thrun, *Probabilistic Robotics*, ACM, 2002.

[14] A. Doucet, N. De Freitas, and N. Gordon, *Sequential Monte Carlo methods in practice*, Springer Verlag, 2001.

[15] M.S. Arulampalam, S. Maskell, N. Gordon, and T. Clapp, "A tutorial on particle filters for online nonlinear/non-Gaussian Bayesian tracking," *IEEE Transactions on signal processing*, vol. 50, no. 2, 2002.

[16] N.J. Gordon, D.J. Salmond, and A.F.M. Smith, "Novel approach to nonlinear/non-Gaussian Bayesian state estimation," in *IEEE Proceedings*, 1993, vol. 140, pp. 107–113.

[17] J. Carlstrom and I. Nygren, "Terrain navigation of the swedish AUV62f vehicle," in *Int. Symp. Unmanned Untethered Submersible Technol. UUST*, Durham, NH, 2005.

[18] B. Jalving, K. Gade, O.K. Hagen, and K. Vestgard, "A toolbox of aiding techniques for the hugin auv integrated inertial navigation system," *Modeling Identification and Control*, vol. 25, no. 3, pp. 173, 2004.

[19] Paul D. Groves, Robin J. Handley, and Andrew R. Runnalls, "Optimising the integration of terrain referenced navigation with INS and GPS," *The Journal of Navigation*, vol. 59, no. 01, pp. 71–89, 2005.

[20] J. Hollowell, "Heli/sitan- a terrain referenced navigation algorithm for helicopters," *IEEE PLANS*, vol. 20, no. 23, pp. 616–625, 1990, SITAN paper.